

# Data-Driven Fault Detection of Vertical Rail Vehicle Suspension Systems

Xiukun Wei

State Key Laboratory of  
Rail Traffic Control and Safety  
Beijing Jiaotong University,  
Beijing 100044, China.  
Email: wwwwkk@gmail.com

Limin Jia

State Key Laboratory of  
Rail Traffic Control and Safety  
Beijing Jiaotong University,  
Beijing 100044, China.  
Email: jialm@vip.sina.com

Hai Liu

School of Traffic and Transportation,  
Beijing Jiaotong University,  
Beijing 100044, China.  
Email: 10121140@bjtu.edu.cn

**Abstract**—This paper concerns data driven fault detection of vertical rail vehicle suspension systems issue. The underlying vehicle system are equipped with only accelerator sensors in the four corners of the carbody, the front and trail bogie, respectively. The faults considered are the vertical damper fault and vertical spring fault. Both PCA-based and CVA-based fault detection methods are studied in this paper. When there is a detectable fault, the detector sends an alarm signal if the residual evaluation is larger than a predefined threshold. By using the professional multi-body simulation tool, SIMPACK, the effectiveness of the proposed approach is demonstrated by simulation results for several fault scenarios.

## I. INTRODUCTION

Suspension systems for rail vehicles are to support the carbody and bogie, to isolate the forces generated by the track unevenness at the wheels, and to control the attitude of the carbody with respect to the track surface for providing ride comfort. The railway vehicle suspension system is very important parts of railway vehicle and the reliability of the suspension system is directly related to the vehicle safety.

On line fault detection and condition monitoring for the suspension system of rail vehicles offer a number of benefits to railway systems/operations. Detection of component faults at their early stages will prevent further deterioration in vehicle performance and enhance vehicle safety. Timely repair or replacement of the faulty components will lead to increased operational reliability and availability. The need for scheduled maintenance and associated costs can be significantly reduced, because maintenance in the future may be carried out on demand. So it is necessary to timely detect the fault of vehicles suspension after it occurs. Some studies on the condition monitoring of railway vehicle and suspension systems are reported in [1],[2],[3], [6], [9], [8]and the references therein.

The fault detection issue of the rail vehicle suspension systems are paid some attentions in the recent years. In [10][11], the authors derived a fault detection approach for the rail vehicle suspension systems based on Kalman filter. The fault isolation is handled by using the similarity measurements. The interaction multi-model (IMM) approach and parameter estimation reported in [4],[6] are convinced to be appropriate alternatives. However, when IMM method is applied, the models needed is increasing very dramatically when more

components in the primary suspension and secondary suspension are considered. Parameter estimation method [6] applies the particles filter for the parameter estimation. The parameter changes are identified online to indicate the health condition of the components. Nevertheless, the computation burden of this approach cannot afforded by the current available monitoring unit. It is true that there is great potential for the improvement in the performance of condition monitoring if the a priori knowledge or information captured by the models is fully used. However, in many cases, the parameters of the vehicle suspension system are not available. In the mean time, due to nonlinearities of the components and the complexities of the suspension systems, a precise model cannot be obtained. Due to these limitations of the model based fault detection approaches, there is increasing interest in using the multivariate statistical approaches to monitoring system health conditions[7][12][5]. As the knowledge of the authors, there is no any report which solves the fault detection problem based on data driven methods.

In this paper, we consider data driven fault detection of rail vehicle systems problem. The underlying vehicle are only equipped with accelerator sensors in the corners of the carbody, the front and trail bogie, which provide the measured signals for the condition monitoring for the vehicle suspension system. The Dynamical Principle Component Analysis (DPCA) and Canonical Variate Analysis (CVA) based approaches are applied for the fault detection problem, respectively. The considered faults are the vertical damper faults and the vertical spring faults of both primary and secondary suspensions. A subway vehicle model is used for the Matlab-Simpack hybrid simulation study in this paper.

This paper is organized in the following. The railway vehicle system, its dynamics and the sensor configuration for the data collection are introduced in Section 2. In the third section, the DPCA and CVA fault detection methods are briefly reviewed. The SIMPACK-Matlab co-simulation results are provided in Section 4. Finally, conclusions are given in Section 5.

## II. THE VERTICAL RAIL VEHICLE SUSPENSION SYSTEMS

### A. The Vehicle Suspension System

A subway vehicle model is used for the study in this paper. To describe the dynamic behaviour more accuracy, three degree-of-freedom (bounce, pitch and roll) is considered for both carbody and bogies. The vertical suspension system of this subway vehicle is depicted in Fig. 1. The equations describing the dynamic behaviour of the railway vehicle are developed from the application of Newton's laws of motion to the individual masses. The dynamical equations of the suspension system for a vehicle moving on a straight track are derived in the following.

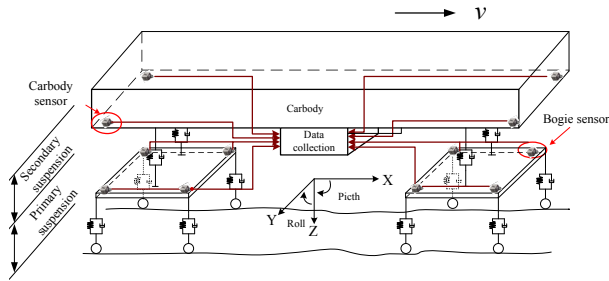


Fig. 1. The vertical suspension system of the rail vehicle

For the carbody, the three DOF equations are described as:

$$\begin{aligned} M\ddot{z} + 4C_{2z}\dot{z} - 2C_{2z}\dot{z}_{FB} - 2C_{2z}\dot{z}_{RB} + 4K_{2z}z \\ - 2K_{2z}z_{FB} - 2K_{2z}z_{RB} = 0 \end{aligned} \quad (1)$$

$$\begin{aligned} J_\phi\ddot{\phi} + 4C_{2z}l^2\dot{\phi} - 2C_{2z}l\dot{z}_{FB} + 2C_{2z}l\dot{z}_{RB} + \\ 4K_{2z}l^2\phi - 2K_{2z}lz_{FB} + 2K_{2z}lz_{RB} = 0 \end{aligned} \quad (2)$$

$$\begin{aligned} J_\theta\ddot{\theta} + 4C_{2z}b^2\dot{\theta} - 2C_{2z}b^2\dot{\theta}_{FB} - 2C_{2z}b^2\theta_{RB} \\ + (4K_{2z}b^2 + 2K_\theta)\theta - (2K_{2z}b^2 + K_\theta)\theta_{FB} \\ - (2K_{2z}b^2 + K_\theta)\theta_{RB} = 0 \end{aligned} \quad (3)$$

Where  $z$ ,  $z_{FB}$  and  $z_{RB}$  are the vertical displacement of the carbody, the leading bogie and the trailing bogie, respectively.  $\phi$  represents the pitch angle of the center of gravity(c.g.) while  $\theta$  is the roll angle of the c.g. for the masses. Their subscripts have the same meaning with the subscripts of  $z$ . Please refer to Table I for the parameters.

For the leading bogie, the three DOF equations are described as:

$$\begin{aligned} M_B\ddot{z}_{FB} - 2C_{2z}\dot{z} - 2C_{2z}l\dot{\phi} + (4C_{1z} + 2C_{2z})\dot{z}_{FB} \\ - C_{1z}\dot{z}_{W1R} - C_{1z}\dot{z}_{W1L} - C_{1z}\dot{z}_{W2R} - C_{1z}\dot{z}_{W2L} - \\ 2K_{2z}z - 2K_{2z}l\phi + (4K_{1z} + 2K_{2z})z_{FB} - K_{1z}z_{W1R} \\ - K_{1z}z_{W1L} - K_{1z}z_{W2R} - K_{1z}z_{W2L} = 0 \end{aligned} \quad (4)$$

TABLE I  
VEHICLE PARAMETERS

	Description	Unit
$M$	Carbody mass	kg
$M_B$	Bogie mass	kg
$J_\phi$	Carbody pitch inertia	$kgm^2$
$J_\theta$	Carbody roll inertia	$kgm^2$
$J_{B\phi}$	Bogie pitch inertia	$kgm^2$
$J_{B\theta}$	Bogie roll inertia	$kgm^2$
$l_b$	Half of the distance between two wheelsets in a bogie	m
$w_b$	Half of the distance between two air spring in lateral	m
$l_c$	Half of the carbody length	m
$w_c$	Half of the carbody width	m
$K_{2z}$	Spring constants of air spring	$kN/m$
$K_{1z}$	Spring constants of primary spring	$kN/m$
$C_{2z}$	Damping constants of secondary damper	$kNs/m$
$C_{1z}$	Damping constants of primary damper	$kNs/m$
$K_\theta$	Spring constants of the anti-roll spring	$kN/m$

$$\begin{aligned} J_{B\phi}\ddot{\phi}_{FB} + 4C_{1z}l_1^2\dot{\phi}_{FB} - C_{1z}l_1\dot{z}_{W1R} - C_{1z}l_1\dot{z}_{W1L} + \\ C_{1z}l_1\dot{z}_{W2R} + C_{1z}l_1\dot{z}_{W2L} + 4K_{1z}l_1^2\phi_{FB} - K_{1z}l_1z_{W1R} \\ - K_{1z}l_1z_{W1L} + K_{1z}l_1z_{W2R} + K_{1z}l_1z_{W2L} = 0 \end{aligned} \quad (5)$$

$$\begin{aligned} J_{B\theta}\ddot{\theta}_{FB} - 2C_{2z}b^2\dot{\theta} + (2C_{2z}b^2 + 4C_{1z}b_1^2)\dot{\theta}_{FB} + \\ C_{1z}b_1\dot{z}_{W1R} - C_{1z}b_1\dot{z}_{W1L} + C_{1z}b_1\dot{z}_{W2R} - C_{1z}b_1\dot{z}_{W2L} \\ - (2K_{2z}b^2 + K_\theta)\theta + (2K_{2z}b^2 + 4K_{1z}b_1^2 + K_\theta)\theta_{FB} + \\ K_{1z}b_1z_{W1R} - K_{1z}b_1z_{W1L} + K_{1z}b_1z_{W2R} - K_{1z}b_1z_{W2L} = 0 \end{aligned} \quad (6)$$

Where  $z_{W1R}$  represents the vertical displacement of the right wheel in the leading wheelset under the leading bogie while  $z_{W2L}$  means the vertical displacement of the left wheel in the trailing wheelset under the leading bogie. The meanings of other symbols can be easily understood in this logic. In consideration of the fact that the wheelsets are rolling against the track, the vertical displacement of the wheel can be seen as the unevenness of the track. In a similar way, the model of the trailing bogie can be derived.

The state-space form of the vehicle dynamical model can be derived as:

$$\dot{x} = Ax + B_d d \quad (7)$$

$$y = Cx + D_d d \quad (8)$$

where

$$x = [\dot{z} \dot{\phi} \dot{\theta} z \phi \theta \dot{z}_{FB} \dot{\phi}_{FB} \dot{\theta}_{FB} z_{FB} \phi_{FB} \theta_{FB}]^T$$

$$d = [\dot{z}_{W1R} \dot{z}_{W1L} \dot{z}_{W2R} \dot{z}_{W2L} z_{W1R} z_{W1L} \dot{z}_{W2R} z_{W2L} \dot{z}_{W3R} \dot{z}_{W3L} z_{W3R} z_{W3L} \dot{z}_{W4R} \dot{z}_{W4L} z_{W4R} z_{W4L}]^T$$

$$y = [z \phi \theta z_{FB} \phi_{FB} \theta_{FB} z_{RB} \phi_{RB} \theta_{RB}]^T$$

Matrixes  $A$ ,  $B_d$ ,  $C$  and  $D_d$  can be derived from the above differential equations,  $d$  is the vertical track velocity and displacement due to track vertical irregularities.

### B. The Model Based on Acceleration Measurements

The developed model (7) and (8) represent the dynamical property of the vehicle suspension system. In this model, the vertical displacement, pitch angle displacement and roll angle displacement of the carbody and the bogie are needed to be measured for the fault detection purpose. However, displacement sensor and angle sensors have the problems such as reliability, maintenance and installation. Compare to these sensors, accelerator sensors have the advantages of cheap and reliable. It does not need to be maintained for a long time period. Due to all the reasons stated above, only accelerator sensors are adopted for obtaining the measurement signals. The sensor configuration is designed as shown in Fig. 1. In the following, the new output equation will be derived.

Carbody sensors are equipped in the four corners on the floorboard, and the bogie sensors are equipped in the four corners on the upside of the bogie. By applying double integral to the acceleration signals, displacement signals are acquired. That is

$$z = \int \int adt dt \quad (9)$$

where  $a$  is the acceleration value and  $z$  is the displacement. However, these displacement signals obtained is different from the outputs in our model, for example, the angle displacements. So, the model outputs needed to be modified.

As depicted in Fig. 2, we set four index points on the rectangle to discuss the relationship between the vertical displacements at the four corners with the angle displacement. These four index points are the center of the rectangle, the middle point of the front edge, the middle point of the right edge and the front corner on the right. The vertical displacement of the four index points are  $z$ ,  $z_F$ ,  $z_R$  and  $z_{FR}$ , respectively. Then one obtains

$$z + z_{FR} = z_F + z_R \quad (10)$$

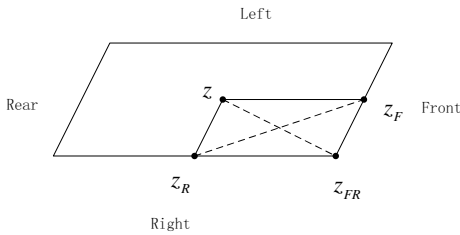


Fig. 2. Relationship among the displacement of the four index points

Consider the pitch motion, we have the equation

$$z_F = z + l \sin(\phi) \approx z + l\phi \quad (11)$$

for a small pitch angle.

Consider the roll motion, we have a similar equation:

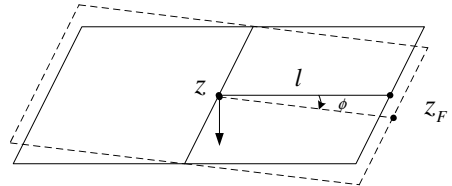


Fig. 3. The pitch motion

$$z_R \approx z - w\theta \quad (12)$$

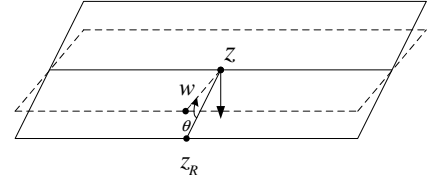


Fig. 4. The roll motion

Combing with (10),(11),(12) together, we have the following transformation relationship:

$$z_{FR} \approx z + l\phi - w\theta \quad (13)$$

In the same procedure, one obtains:

$$z_{FL} \approx z + l\phi + w\theta \quad (14)$$

$$z_{RR} \approx z - l\phi - w\theta \quad (15)$$

$$z_{RL} \approx z - l\phi + w\theta \quad (16)$$

Then the new state space is transformed into

$$\dot{x} = Ax + B_d d \quad (17)$$

$$y_{cor} = TCx + TD_d d \quad (18)$$

where the transformation matrix

$$T = \begin{bmatrix} 1 & l_c & -w_c & 0 & 0 & 0 & 0 & 0 & 0 \\ 1 & l_c & w_c & 0 & 0 & 0 & 0 & 0 & 0 \\ 1 & -l_c & -w_c & 0 & 0 & 0 & 0 & 0 & 0 \\ 1 & -l_c & w_c & 0 & 0 & 0 & 0 & 0 & 0 \\ 0 & 0 & 0 & 1 & l_b & -w_b & 0 & 0 & 0 \\ 0 & 0 & 0 & 1 & l_b & w_b & 0 & 0 & 0 \\ 0 & 0 & 0 & 1 & -l_b & -w_b & 0 & 0 & 0 \\ 0 & 0 & 0 & 1 & -l_b & w_b & 0 & 0 & 0 \\ 0 & 0 & 0 & 0 & 0 & 0 & 1 & l_b & -w_b \\ 0 & 0 & 0 & 0 & 0 & 0 & 1 & l_b & w_b \\ 0 & 0 & 0 & 0 & 0 & 0 & 1 & -l_b & -w_b \\ 0 & 0 & 0 & 0 & 0 & 0 & 1 & -l_b & w_b \end{bmatrix}$$

where

$$y_{cor} = [z_{FR} \ z_{FL} \ z_{RR} \ z_{RL} \ z_{FB\_FR} \ z_{FB\_FL} \ z_{FB\_RR} \ z_{FB\_RL} \ z_{RB\_FR} \ z_{RB\_FL} \ z_{RB\_RR} \ z_{RB\_RL}]^T$$

$z_{FR}$  and  $z_{FL}$  represent the vertical displacement of the front corners on the right and left, respectively.  $z_{FBFR}$  represent the vertical displacement of the front corner on the right of the leading bogie.

*Remark 2.1:* Data is the very critical for the data driven fault detection methods. The data should contain rich information of the system dynamics and the fault information when a fault occurs in the system. In this paper, only acceleration sensors are used for the vehicle suspension fault detection systems. From the above observation, the dynamics of rail vehicle suspension systems are contained in the displacements of the the carbody, the front and rail bogies, which can be obtained by the acceleration sensors. The sensor configuration presented before can provided enough information for the fault detection.

### III. DPCA AND CVA FAULT DETECTION PRINCIPLE

Thanks to its simplicity and efficiency in processing huge amount of process data, PCA is recognized as a powerful tool of statistical process monitoring and widely used in the process industry for purpose of fault detection and diagnosis[12][7]. In the meantime, it is noticed that the CVA based condition monitoring methods are outperformed PCA based approaches [5]. In this paper, both methods are studied for the considered vehicle suspension fault detection systems. The main steps for these two methods are briefly reviewed in this section.

#### A. A Brief Description of PCA

The standard PCA-based fault detection consists of three steps and can be formulated as follows:

• Data collection and pre-processing: Consider a data matrix  $X \in \mathbf{R}^{N \times m}$  consisting of  $N$  samples and  $m$  sensors collected from process. Matrix  $X$  is then scaled to zero mean, and often to unit variance. Let the scaled data be

$$\mathbf{Y} = \begin{bmatrix} y_1^T \\ \vdots \\ y_N^T \end{bmatrix} \in \mathbf{R}^{N \times m} \quad (19)$$

with  $y_i \in R^m$ ,  $i = 1, \dots, N$ , denoting the  $i$ th scaled vector.

• Decomposition of covariance matrix: The covariance matrix is formed as

$$\sum_0 \approx \frac{1}{N} \mathbf{Y}^T \mathbf{Y}.$$

By means of SVD or EVD (eigen value decomposition), the covariance matrix is decomposed as follows:

$$\frac{1}{N-1} \mathbf{Y}^T \mathbf{Y} = \mathbf{P} \Lambda \mathbf{P}^T, \Lambda = \begin{bmatrix} \Lambda_{pc} & 0 \\ 0 & \Lambda_{res} \end{bmatrix} \quad (20)$$

with  $\sigma_i^2$ ,  $i = 1, \dots, m$ , is the  $i$ th singular value of the covariance matrix and

$$\begin{aligned} \Lambda_{pc} &= diag(\sigma_1^2, \dots, \sigma_l^2), \Lambda_{res} = diag(\sigma_{l+1}^2, \dots, \sigma_m^2) \\ \sigma_1^2 \geq \dots \geq \sigma_l^2 &\gg \sigma_{l+1}^2 \geq \dots \geq \sigma_m^2, \mathbf{P} \mathbf{P}^T = \mathbf{I}_{m \times m} \\ \begin{bmatrix} \mathbf{P}_{pc}^T \\ \mathbf{P}_{res}^T \end{bmatrix} \begin{bmatrix} \mathbf{P}_{pc} & \mathbf{P}_{res} \end{bmatrix} &= \begin{bmatrix} \mathbf{I}_{l \times l} & 0 \\ 0 & \mathbf{I}_{(m-l) \times (m-l)} \end{bmatrix} \end{aligned}$$

• On-line fault detection: When a new scaled measurement  $x \in \mathbf{R}^m$  is available, the SPE and Hotelling's  $T^2$  indices can be computed as

$$\mathbf{T}^2 = y^T \mathbf{P}_{pc} \Lambda_{pc}^{-1} \mathbf{P}_{pc}^T y \quad (21)$$

$$SPE = y^T \mathbf{P}_{res} \mathbf{P}_{res}^T y \quad (22)$$

The fault detection logic is  $SPE \leq J_{th,SPE}$  and  $T^2 \leq J_{th,T^2} \Rightarrow$  fault-free. Otherwise  $\Rightarrow$  faulty.

where  $J_{th,T^2}$  and  $J_{th,SPE}$  are the thresholds for SPE and  $T^2$  respectively.

The PCA methods can be extended to take into account the serial correlations, by augmenting each observation vector with the previous  $l$  observations and stacking the data matrix in the following manner,

$$\mathbf{Y}(l) = \begin{bmatrix} y_t^T & y_{t-1}^T & \cdots & y_{t-l}^T \\ y_{t-1}^T & y_{t-2}^T & \cdots & y_{t-l-1}^T \\ \vdots & \vdots & \ddots & \vdots \\ y_{t+l-n}^T & y_{t+l-n-1}^T & \cdots & y_{t-n}^T \end{bmatrix} \quad (23)$$

where  $y_t^T$  is the  $m$ -dimensional observation vector in the training set at time instance  $t$ . By performing PCA on the data matrix in Eq. 23, a multivariate autoregressive (AR) (ARX model if the process inputs are included) is extracted directly from the data. This approach of applying PCA to Eq. 23 is referred to here as dynamic PCA (DPCA).

#### B. CVA for Dynamic Processes

The stacked past and future vectors,  $\mathbf{p}$  and  $\mathbf{f}$ , are represented as follows:

$$\mathbf{p}_{t-1}^{t-l} = [\mathbf{y}_{t-1}^T \cdots \mathbf{y}_{t-l}^T]^T \quad (24)$$

$$\mathbf{f}_t^{t+l+1} = [\mathbf{y}_t^T \cdots \mathbf{y}_{t+l-1}^T]^T \quad (25)$$

where  $\mathbf{y}$  denotes output vectors, subscript  $t$  is the present time index for  $\mathbf{y}$ , and  $l$  is the number of the lag or the lead. In CVA, the stacked future and past vectors are normalized using

$$\mathbf{d}_{f,t} = \sum_{ff}^{-1/2} \mathbf{f}_t^{t+l+1}, \mathbf{d}_{p,t-1} = \sum_{pp}^{-1/2} \mathbf{p}_{t-1}^{t-l} \quad (26)$$

where  $\sum_{ff} = E(\mathbf{f}_t^{t+l+1} \mathbf{f}_t^{t+l+1 T})$  and  $\sum_{pp} = E(\mathbf{p}_{t-1}^{t-l} \mathbf{p}_{t-1}^{t-l T})$  ( $E(\cdot)$  denotes the expectation operator). The normalized vectors  $\mathbf{d}_{f,t}$  and  $\mathbf{d}_{p,t-1}$  are defined as the scaled stacked future and past vectors at time  $t$ , respectively. The conditional expectation of the scaled future vector takes the form:

$$\hat{E}(\mathbf{d}_{f,t} | \mathbf{d}_{p,t-1}) = \sum_{ff}^{-1/2} \sum_{fp} \sum_{pp}^{-1/2} \mathbf{d}_{p,t-1} \quad (27)$$

where  $\hat{E}(\alpha | \beta)$  denotes the expectation of  $\alpha$  under condition  $\beta$ . The physical mean of  $\sum_{fp}$ , defined as  $E(\mathbf{f}_t^{t+l+1} \mathbf{p}_{t-1}^{t-l T})$ , is the well-known Hankel matrix. Thus,  $\sum_{ff}^{-1/2} \sum_{fp} \sum_{pp}^{-1/2}$  indicates the scaled Hankel matrix. The scaled Hankel matrix can be factorized using singular value decomposition (SVD),

$$\begin{aligned} \widehat{\mathbf{d}}_{f,t} &= \sum_{ff}^{-1/2} \sum_{fp} \sum_{pp}^{-1/2} \mathbf{d}_{p,t-1} \\ &= \mathbf{U} \mathbf{S} \mathbf{V}^T \mathbf{d}_{p,t-1} \approx \mathbf{U}_k \mathbf{S}_k \mathbf{V}_k^T \mathbf{d}_{p,t-1} \end{aligned} \quad (28)$$

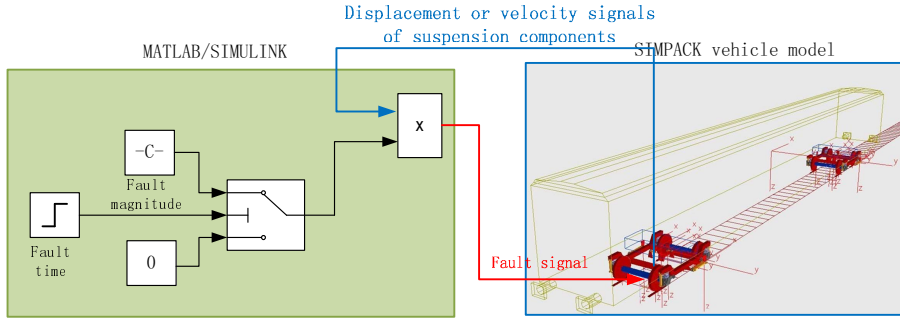


Fig. 5. Co-simulation between SIMPACK and MATLAB/SIMULINK

where  $\hat{\mathbf{d}}_{f,t}$  denotes  $\hat{E}(\mathbf{d}_{f,t}|\mathbf{d}_{p,t-1})$  and  $k$  represents the state order.  $\mathbf{U}_k$  and  $\mathbf{V}_k$  consist of the first  $k$  column vectors of  $U$  and  $V$ , respectively, and the diagonal matrix  $\mathbf{S}_k$  is the  $k \times k$  principal submatrix of  $\mathbf{S}$ . Then, the past and future CVs at time  $t$  are given by

$$\begin{aligned}\mathbf{z}_t &= \mathbf{U}_k^T \mathbf{d}_{f,t} = \mathbf{U}_k^T \sum_{ff}^{-1/2} \mathbf{f}_t^{t+l+1} = \mathbf{L}_k \mathbf{f}_t^{t+l+1} \\ \mathbf{m}_t &= \mathbf{V}_k^T \mathbf{d}_{p,t-1} = \mathbf{V}_k^T \sum_{pp}^{-1/2} \mathbf{p}_{t-1}^{t-l} = \mathbf{J}_k \mathbf{p}_{t-1}^{t-l}\end{aligned}\quad (29)$$

respectively, and these CVs satisfy

$$\mathbf{z}_k = \mathbf{S}_k \mathbf{m}_t \quad (30)$$

Similar to the  $T^2$  and SPE indices, the following indices are used in this paper:

$$T_s^2 = \mathbf{y}^T \mathbf{J}_k \mathbf{J}_k^T \mathbf{y} \quad (31)$$

$$SPE_s = r_t^T r_t \quad (32)$$

where  $r_t = (\mathbf{I} - \mathbf{J}_k \mathbf{J}_k^T) \mathbf{y}$

## IV. SIMULATION

### A. Co-simulation to Generate the Suspension Faults

In this section, SIMPACK vehicle model is used to generate the acceleration signals and different faults in both primary and secondary suspension are simulated. Here we discuss how to simulate the suspension faults in SIMPACK. The interface between MATLAB/SIMULINK and SIMPACK make it possible to simulate suspension fault with different fault magnitudes at any time during the operation.

As we all known, the damper will generate a force, whose value equals the damper coefficient times piston's velocity, to reject the moving of the piston. And we generate the damper fault signal in the way it works. As shown in Fig. 5, for example, sensors are equipped at the position of a secondary damper to measure it's moving velocity. Suggest that the damper lose half of its value at the 15th second. Then a external force is exerted on the piston to reduce the performance of the damper as shown in Fig. 5. The direction of the external force is opposite to the force generated by the damper, and the value of force equals the fault magnitude times piston's velocity. In a similar way, spring fault can be simulated.

TABLE II  
FAULT SCENARIOS

scenario	fault	fault pattern	faulty time (s)
fault 0	no fault		
fault 1	$C_2$	failure	15
fault 2	$K_1$	lost 90%	20
fault 3	$K_2$	lost 25%	30
fault 4	$K_2$	lost 90%	30

### B. Fault Detection Results

The simulation results for the railway vehicle suspension fault detection are shown in this section. The track irregularities used in the simulations are the German 6th grade track spectrum. The faults considered in the simulation study are listed in Table II.

The no fault data are used for training the models. For the DPCA approach, the time lags is selected as 20. 120 principle components are selected to be retained in the model. For the CVA approach, the measured data is compressed by PCA method and only 6 variables are kept in the new data. This avoids the problem that  $\Sigma_{ff}^{-1/2}$  and  $\Sigma_{pp}^{-1/2}$  are not real. The time lags and leads in the CVA approach are selected as 20. In the CVA model, 18 states are selected.

The fault detection results are shown in Fig. 6-9. In all the figures, the red solid line indicates the no fault case. The blue dashed line represents the case of  $C_2$  failure. The  $K_1$  lost 90% of its value is indicated by the green dash-dotted line. For the fourth scenario,  $K_1$  lost 25% of its value, is represented by the black dotted line. Finally, the  $K_1$  lost 90% of its value fault is represented by the cyan dots.

Fig. 6 shows the fault detection results of PCA approach using the  $T^2$  index. Fault 1, 2 and 4 are detected successfully. The  $T^2$  index of the weak fault 3 is not obvious. The SPE index of the PCA approach is shown in Fig. 7. The performance is similar to that of the  $T^2$  index. Fig. 8 shows the results of the CVA approach by using  $T_s^2$  index. It can be seen that the CVA approach is very sensitive to fault 2. The fault 1 is also detected successfully. The detection results of the fault 3 and 4 are not very satisfied. Similar performance is observed by using the  $SPE_s$  index.

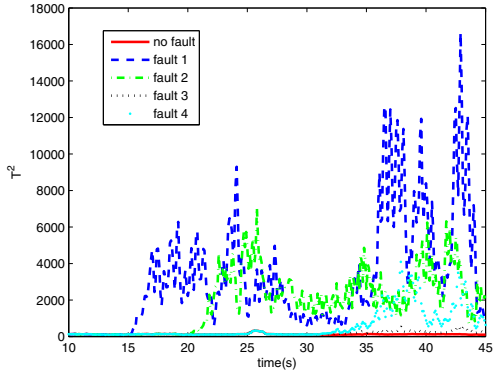


Fig. 6. Fault detection results based on PCA and  $T^2$  index

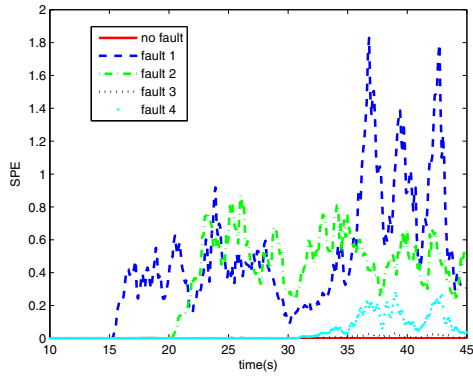


Fig. 7. Fault detection results based on PCA and  $SPE$  index

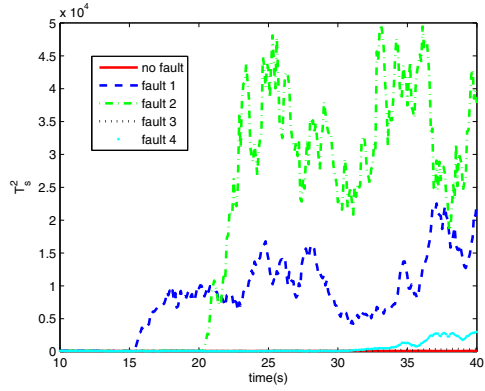


Fig. 8. Fault detection results based on CVA and  $T_s^2$  index

## V. CONCLUSION

In this paper, the data driven fault detection problem for the railway vehicle suspension systems are studied. A new fault detection system is proposed where only the acceleration signals are used for the detection purpose. Both PCA and CVA based approaches are studied. For large magnitude faults, both approaches achieves very good detection performance. However, for weak faults, for instance, the  $K_2$  lost of 25% of its value, both methods do not detect the faults obviously. This means that both methods cannot detect early stage fault. New strategy for improving the sensitivity of the data driven fault detection methods are necessary. The final comment is that the

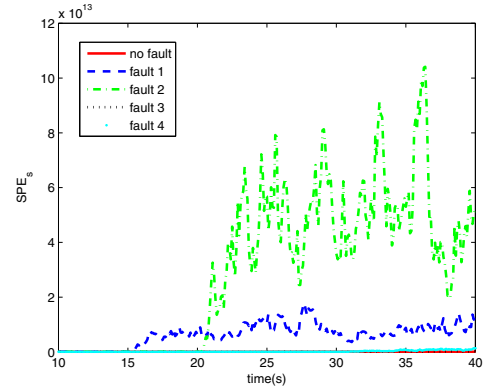


Fig. 9. Fault detection results based on PCA and  $SPE_s$  index

components nonlinearities are not considered in the simulation study. They should be investigated in the future work.

## ACKNOWLEDGMENT

This work is partly supported by Chinese 863 program (Contract No. 2011AA110503-6), State Key Laboratory of Rail Traffic Control and Safety (Contract No.RCS2011ZZ005) and Ph.D. Programs Foundation of Ministry of Education of China (grant number: 20110009120037).

## REFERENCES

- [1] S. Bruni, R. Goodall, T. X. Mei, and H. Tsunashima, "Control and monitoring for railway vehicle dynamics," *Vehicle System Dynamics*, vol. 45, no. 7-8, pp. 765–771, 2007.
- [2] R. Goodall and T. Mei, "Advanced control and monitoring for railway vehicle suspensions," in *International Symposium on Speed-up and Service Technology for Railway and Maglev Systems(STECH'06)*, Chengdu,China, 1 2006, pp. 10–16.
- [3] R. Goodall and C. Roberts, "Concepts and techniques for railway condition monitoring," in *IET International Conference on Railway Condition Monitoring*, 2006, pp. 90–95.
- [4] Y. HAYASHI, H. TSUNASHIMA, and Y. MARUMO, "Fault dectecion of railway vehicle suspension systems using multiple-model approach," *Mechanical System for Transportation and Logistics*, vol. 1, no. 1, pp. 88–98, September 2008.
- [5] C. Lee, S. W. Choi, and L. In-Beum, "Variable reconstruction and sensor fault identification using canonical variate analysis," *Journal of Process Control*, vol. 16, pp. 747–761, 2006.
- [6] P. Li, R. Goodall, P. Weston, C. S. Ling, C. Goodman, and C. Roberts, "Estimation of railway vehicle suspension parameters for condition monitoring," in *Control Engineering Practice*, 2006, pp. 43–55.
- [7] S. J. Qin, "Data-driven fault detection and diagnosis for complex industrial processes," in *The 7th IFAC Symposium on Fault Detection, Supervision and Safety of Technical Processes*, Barcelona,Spain, 2009, pp. 1115–1125.
- [8] X. Wei, L. Jia, and H. Liu, "Fault diagnosis filter design for railway vehicle suspension systems based on lmi optimization," *An international Interdisciplinary Journal*, vol. accepted, 2012.
- [9] X. Wei, S. Lin, and H. liu, "Distributed fault detection observer for rail vehicle suspension systems," in *Chinese Control and Decision Conference*, accepted, 2012.
- [10] X. Wei, H. liu, and Y. Qin, "Fault diagnosis of rail vehicle suspension systems by using GLRT," *Chinese Control and Decision Conference*, 2011.
- [11] —, "Fault isolation of rail vehicle suspension systems by using similarity measure," in *International Conference on Intelligent Railway Tranportation*, Bei Jing, China, 2011, pp. 391–396.
- [12] S. Yin, S. Ding, A. Naik, P. Deng, and A. Haghani, "On pca-based fault diagnosis techniques," in *2010 Conference on control and Fault Tolerant Systems*, Nice,France, 2010, pp. 179–184.